Organic Geochemistry 56 (2013) 40–50

Contents lists available at SciVerse ScienceDirect

Organic Geochemistry

journal homepage: www.elsevier.com/locate/orggeochem

Microbial glycerol dialkyl glycerol tetraethers from river water and soil near the Three Gorges Dam on the Yangtze River

Guifang Yang [a,*], Chuanlun L. Zhang [b,c,*], Shucheng Xie [d], Zhenghong Chen [e], Meiling Gao [a], Zhiliang Ge [a], Zhen Yang [a]

[a] School of Earth Sciences and Resources, China University of Geosciences, Beijing 100083, China
[b] State Key Laboratory of Marine Geology, Tongji University, Shanghai 200092, China
[c] Department of Marine Sciences, University of Georgia, Athens, GA 30602, USA
[d] State Key Laboratory of Biogeology and Environmental Geology, China University of Geosciences, Wuhan 430074, China
[e] China Meteorological Administration Training Centre, Beijing 100081, China

ARTICLE INFO

Article history:
Received 11 June 2012
Received in revised form 26 November 2012
Accepted 30 November 2012
Available online 10 December 2012

ABSTRACT

Suspended particulate matter (SPM) was collected above and below the Three Gorges Dam (TGD) on the Yangtze River in May, July and December 2009, respectively, for a study of the spatial and temporal variation in glycerol dialkyl glycerol tetraethers (GDGTs) in the riverine system. The branched GDGTs (*b*GDGTs) were > 0.6 ng/l and isoprenoid GDGTs (*i*GDGTs) > 0.3 ng/l in most SPM samples in May and July, whereas, *i*GDGTs were on average about 10× more abundant than *b*GDGTs in December. The results suggest that the abundance of *b*GDGTs and *i*GDGTs in the Yangtze River at the TGD varied seasonally, which might be affected by soil runoff and in situ production. Despite these effects, the TEX_{86}-inferred temperature derived from SPM reflected the measured river surface water temperature in the sampling months, suggesting that planktonic *Thaumarchaeota* might actively make *i*GDGTs in the river water near the TGD throughout the year. The *b*GDGT-derived CBT/MBT temperature from the SPM was not significantly different among the three seasons and the values together averaged 15.2 ± 0.7 °C, close to the annual mean air temperature (16.9 °C) in the region near the TGD. However, the *b*GDGT-derived pH_{CBT} values were close to the water pH and slightly higher than the pH of the local soil. These results suggest that the sources of *b*GDGTs in the river water are complicated and that *b*GDGTs may not solely derive from the local soil runoff. Nevertheless, our study highlights the potential of using TEX_{86} and MBT/CBT proxies for a better understanding of the source and mechanism of GDGT production in riverine systems increasingly affected by the construction of dams.

1. Introduction

Rivers are commonly viewed as conduits transporting terrestrial material from land to the ocean (Milliman and Syvitski, 1992; Walling and Fang, 2003; Chen and Saito, 2011). However, mounting evidence indicates that climate change and increasing anthropogenic activity may alter the river hydrological cycle and ecosystem by affecting the pattern of sedimentation or composition of the microbial community in the river (Colloschonn et al., 2001; Herfort et al., 2006; Yang et al., 2007; Kim et al., 2012). For instance, dams may interrupt the flow behavior of river water and create hydrologically dynamic reservoirs that change biogeochemical terrestrial signals, possibly affecting the interpretation of the signals in river catchments (Xu and Milliman, 2009).

Our knowledge of how anthropogenic behavior and seasonal climate impact terrestrial input, transport and associated eco-environmental variation in big-river basins is based primarily on the proxy indicators in environmental archives, such as micropaleontology and analysis of marine and lacustrine sediments (Millman and Meade, 1983; Meyers, 1994; Kim et al., 2007; Walsh et al., 2008; Chen and Saito, 2011). Recently, a number of new proxies based on glycerol dialkyl glycerol tetraethers (GDGTs) have been shown to reflect terrestrial environmental signals and palaeoclimatic variation (Sinninghe Damsté et al., 2000; Schouten et al., 2002; Weijers et al., 2007a,b; Kim et al., 2010; Xie et al., 2012). A comprehensive recent review on GDGTs is given by Schouten et al. (2013).

GDGTs exist in two forms (Fig. 1): isoprenoid (*i*GDGTs) and branched (*b*GDGTs). *i*GDGT membrane lipids have been found predominantly in peat bogs (Pancost et al., 2000; Schouten et al., 2000; Pancost and Sinninghe Damsté, 2003; Weijers et al., 2004), and marine and lacustrine waters and sediments (Schouten et al., 2000; Powers et al., 2004; Sun et al., 2011; Wang et al., 2012). In

* Corresponding authors.
E-mail addresses: yangguifang@cugb.edu.cn (G.F. Yang), archaea.zhang@gmail.com (C.L. Zhang).

0146-6380/$ - see front matter © 2012 Elsevier Ltd. All rights reserved.
http://dx.doi.org/10.1016/j.orggeochem.2012.11.014

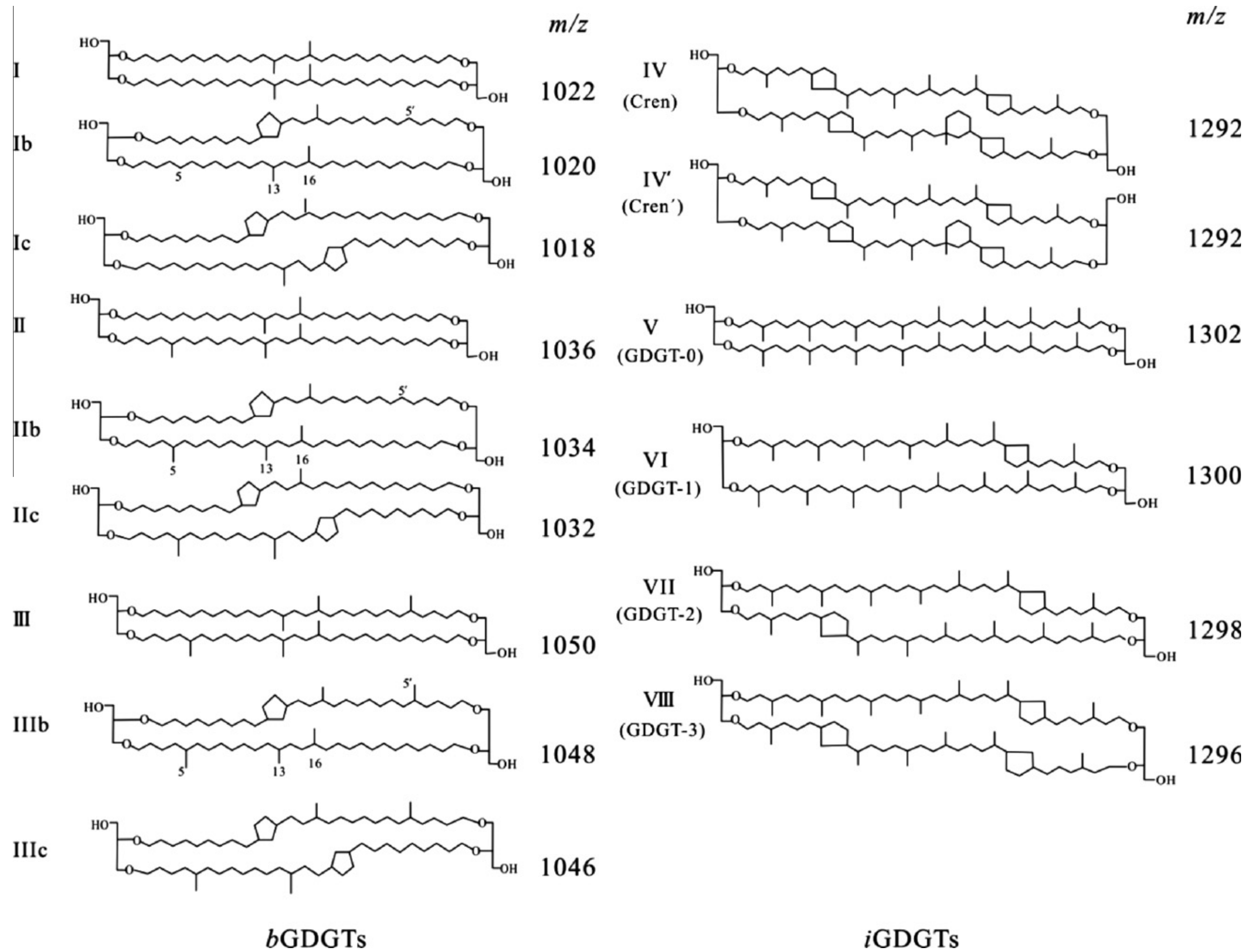

Fig. 1. Structures of bacterial GDGTs (*b*GDGTs) and archaeal isoprenoid GDGTs (*i*GDGTs).

aquatic environments, the *i*GDGT lipids are most likely derived from pelagic *Crenarchaeota* (i.e. group 1.1 *Crenarchaeota*; DeLong, 1998), which are now assigned as *Thaumarchaeota* (Brochier-Armanet et al., 2008; Pester et al., 2011). Based on the relative distribution of membrane lipids derived from planktonic *Thaumarchaeota*, the TEX_{86} paleothermometer has been widely applied to both marine and lacustrine environments for surface temperature estimation in both oceanic (Schouten et al., 2002, 2003; Wuchter et al., 2004; Kim et al., 2008) and lacustrine environments (Powers et al., 2004, 2010; Pearson et al., 2011).

Another recently recognized group of GDGTs, containing branched (*b*GDGTs) instead of isoprenoid alkyl chains, is ubiquitous in peat (Sinninghe Damsté et al., 2000; Weijers et al., 2006a), soils (Weijers et al., 2007b), lake sediments (Powers et al., 2004, 2010; Blaga et al., 2009) and estuarine and ocean margin sediments (Weijers et al., 2007a,b; Schouten et al., 2008; Rueda et al., 2009; Bendle et al., 2010; Zhang et al., 2012). The MBT/CBT proxy has been applied to infer continental air temperature (Weijers et al., 2007a,b; Sinninghe Damsté et al., 2009; Tierney and Russell, 2009; Zink et al., 2010). It quantifies the degree of cyclisation of branched tetraethers (CBT) and the extent of methylation of branched tetraethers (MBT). CBT correlates with soil pH, whereas MBT responds to soil pH and air temperature (Weijers et al., 2007b; Peterse et al., 2012).

A branched and isoprenoid tetraether (BIT) index has been used as a tracer for soil terrestrial input to the ocean or lake from rivers (Hopmans et al., 2004), with high BIT values indicating high soil input relative to marine production. The index has been widely used in a number of continental margin studies (Herfort et al., 2006; Walsh et al., 2008; Weijers et al., 2009; Smith et al., 2012) and shows potential for estimating the relative amount of soil-derived organic carbon contributed from land to ocean via rivers and for reconstruction of past river discharge (Ménot et al., 2006; Weijers et al., 2009; Kim et al., 2012). The results also suggest that flooding events might play an important role in delivering terrestrial organic matter (OM) to the sea (Kim et al., 2007). On the other hand, a study of suspended particulate matter (SPM) in the Pearl River and estuary showed aquatic production of *b*GDGTs (Zhang et al., 2012) and a study of surface sediments from the Lower Yangtze River and East China Sea revealed the multiple sources and complex shelf processes that govern the distribution of GDGTs (Zhu et al., 2011). In situ production of *b*GDGTs in lacustrine environments has also been reported (e.g. Tierney et al., 2010, 2012; Wang et al., 2012).

Despite these promising results, many issues concerning the proxies remain to be resolved. First, the BIT proxy has been applied primarily to estuaries and some rivers (cf. Herfort et al., 2006; Kim et al., 2007, 2012) and its applicability to larger river environments, the Yangtze River for instance, has not been fully assessed. In the Yangtze basin, the increase in dam building in recent decades may have potentially influenced the BIT and MBT/CBT proxies by creating a "reservoir effect". Furthermore, TEX_{86} has been widely applied as a paleothermometer to marine and lacustrine systems (Powers et al., 2004, 2010; Weijers et al., 2007a), but not to river catchments where the influence of the external input of isoprenoid GDGTs might vary in different seasons. Also, integrated MBT–CBT and TEX_{86} proxies for estimating water temperature and air temperature from the same environment have not been discussed.

We have analyzed the isoprenoid and branched GDGT distributions in SPM from different water depths above and below the Three Gorges Dam (TGD) to evaluate the impact of the dam on riverine processes and the underlying seasonal variation in BIT, MBT/CBT and TEX_{86}. Soil samples from along the flanks of the Yangtze River at the TGD were also analyzed for GDGTs to constrain the source of riverine GDGTs.

2. Material and methods

2.1. Study area and sampling

The TGD is a hydroelectric dam that spans the Yangtze River near the town of Sandouping in Yichang, Hubei province. It is the world's largest power station in terms of installed capacity (21,000 MW). The TGD area is typically subtropical, receiving an annual average precipitation of 1200 mm, with an annual average temperature of 16.9 °C (Chen et al., 2001; Jiang, 2007). The precipitation arrives from the East Asian summer monsoon, with 80% occurring between June and September (Chen et al., 2001).

A total of 27 SPM samples was collected from the river at the TGD area in May, July and December, 2009 (Fig. 2, Table 1). They were collected from four locations (Fig. 2): two above the dam (HR, head of reservoir; CR, central reservoir) and two below the dam (BCD, below and close to the dam; BAD, below and away from the dam) (Fig. 2). The distance between the two locations above the dam was ca. 10 km and 3–4 km between the two locations below the dam. Samples were taken at 5 m, 15 m or 25 m water depth. The water was filtered through a 0.7 μm glass fiber filter for collection of SPM. Three surface soil samples overlying the flanks of the river were also collected. All samples were frozen immediately in liquid N_2 after collection and stored at −20 °C until analysis.

Water temperature was recorded using a Hg thermometer and pH was measured using a Hach pH meter (Hach Company, Loveland, CO, USA). Details of the local climate were recorded. For measuring pH, each dry soil sample was mixed with ultrapure water in a ratio of 1:2.5 (g/ml). The mixture was stirred and allowed to stand (ca. 30 min). The pH values of the supernatant were measured in triplicate by using a pH meter with a precision of ± 0.01.

2.2. Lipid extraction

Soil samples were freeze dried and homogenized with a mortar and pestle. One of the filters was cut into equal pieces with sterile scissors and collected into 50 ml centrifuge tubes. The filter material or 5 g dry soil were extracted by way of gradient sonication (10 min, 3×) with MeOH, dichloromethane (DCM)/MeOH (1:1, v/v) and DCM, respectively. The supernatants were filtered through 0.45 μm glass fiber filters and pooled. The total extract was separated into neutral and polar fractions via Al_2O_3 column chromatography, eluting with hexane:DCM (9:1, v/v) and DCM:MeOH (1:1,v/v), respectively. The polar lipids, containing GDGTs, were filtered through a 0.45 μm glass fiber syringe filter and dried under N_2. No GDGTs were detected in the neutral fraction.

2.3. GDGT analysis

Dried polar fractions were dissolved in hexane:isopropanol (99:1, v/v) and a synthesized C_{46} GDGT was added as internal standard, having a detection limit of 0.8 pg, as described by Huguet et al. (2006). Analysis was performed using high performance liquid chromatography–atmospheric pressure chemical ionization-mass spectrometry (HPLC–APCI-MS) with an Agilent 1200 series liquid chromatograph equipped with an automatic injector and coupled to a QQQ 6460 MS instrument and using Mass Hunter LC–MS manager software with a procedure modified from Hopmans et al. (2004) and Schouten et al. (2007). Separation was achieved with a Prevail Cyano column (2.1 mm × 150 mm, 3 μm; Alltech Deerifled, IL, USA) at 40 °C. Injection volume was 5 μl. GDGTs were first eluted isocratically with 90% A and 1% B for 5 min, followed by a linear gradient to 18% B in 45 min. Solvent was held for 10 min in 100% B and was then allowed to re-equilibrate to 90% A:10% B over 10 min, where A was *n*-hexane and B *n*-hexane/isopropanol

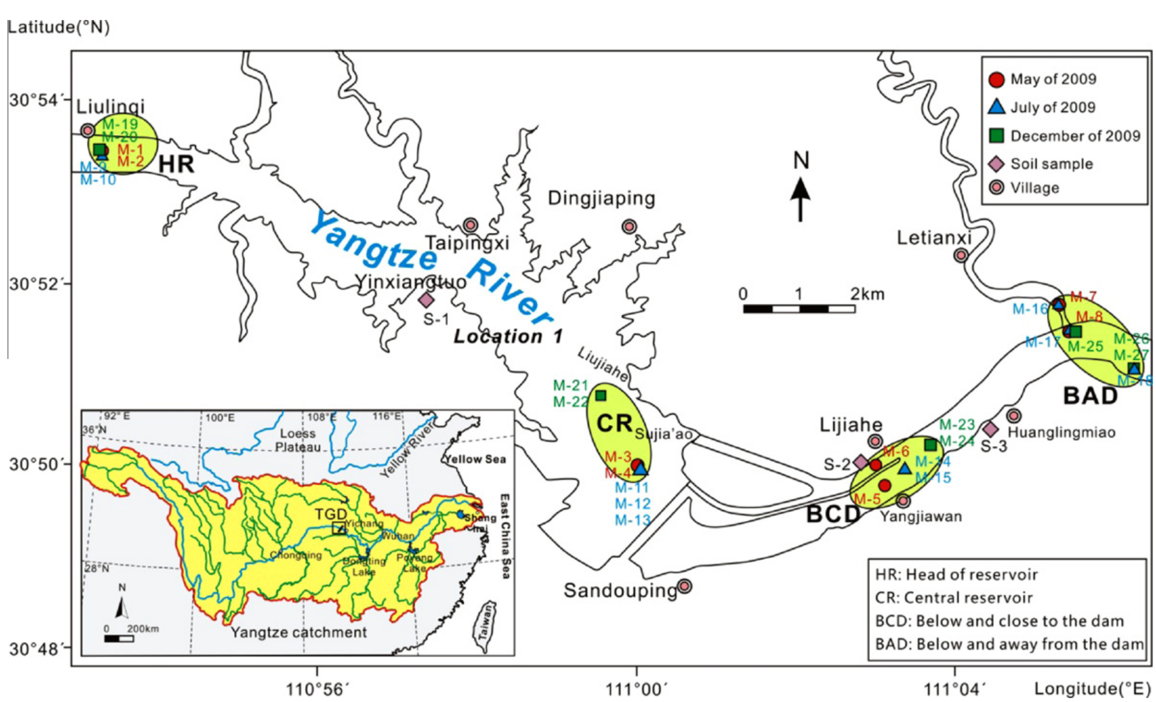

Fig. 2. Map of Three Gorges Dam (TGD) showing location of water and soil samples.

Table 1
Summary of sample locations and GDGT-derived proxies (ID, sample number; ND, not detected).

Season	Location	ID	Depth (m)	*b*GDGTs (ng/l)	*i*GDGTs (ng/l)	Total GDGTs (ng/l)	*b*GDGT/*i*GDGT	BIT	TEX_{86}	MBT	CBT	Actual pH	CBT pH	Actual T (°C)	TEX_{86} Temp (°C)	MBT/CBT Temp (°C)
May-2009	HR	M-1	5	0.7	0.3	1.0	2.20	0.86	0.66	0.47	0.38	8.0	7.8	23.0	22.4	13.9
		M-2	25	3.2	0.8	4.0	3.92	0.92	0.68	0.72	0.44	8.0	7.6	22.0	23.5	25.6
	CR	M-3	5	0.7	0.5	1.2	1.45	0.79	0.64	0.46	0.38	8.0	7.8	19.5	21.3	13.5
		M-4	25	0.1	0.1	0.2	1.74	0.90	0.73	0.59	0.44	8.0	7.6	22.0	26.3	19.0
	BCD	M-5	5	0.2	0.1	0.3	1.47	0.80	0.64	0.53	0.46	8.0	7.5	18.0	21.3	16.1
		M-6	5	0.9	0.3	1.2	2.90	0.88	0.54	0.46	0.35	8.3	7.9	20.8	15.8	13.6
	BAD	M-7[a]	2.5	0.6	0.3	0.9	1.99	0.81	0.67	0.45	0.43	8.0	7.6	22.2	23.0	12.3
		M-8[b]	5	0.3	0.1	0.4	1.81	0.85	0.68	0.51	0.39	8.0	7.7	19.2	23.5	15.8
July-2009	HR	M-9	5	ND	ND	ND	–	0.90	0.69	0.48	0.37	7.9	7.8	27.3	24.1	14.6
		M-10	25	5.2	1.5	6.7	3.57	0.91	0.69	0.51	0.39	7.8	7.8	27.2	24.1	15.7
	CR	M-11	5	0.7	0.2	0.9	3.07	0.90	0.64	0.50	0.38	8.1	7.8	25.0	21.4	15.5
		M-12	15	6.4	2.2	8.6	2.88	0.89	0.73	0.48	0.44	8.1	7.6	24.8	26.3	13.8
		M-13	25	2.2	0.9	3.1	2.40	0.87	0.72	0.39	0.29	8.0	8.0	25.1	25.7	10.8
	BCD	M-14	5	12.3	3.4	15.7	3.58	0.91	0.72	0.45	0.39	8.1	7.7	27.6	25.7	12.9
		M-15	15	9.3	15.2	24.5	0.61	0.50	0.69	0.46	0.38	8.2	7.8	27.6	24.1	13.4
	BAD	M-16[a]	3	2.2	0.5	2.7	4.83	0.93	0.66	0.70	0.54	7.9	7.4	27.6	22.4	23.7
		M-17[b]	5	2.7	0.8	3.5	3.23	0.89	0.73	0.45	0.43	7.9	7.6	27.9	26.3	12.4
		M-18	5	2.6	0.8	3.4	2.98	0.90	0.75	0.46	0.42	8.1	7.7	29.0	27.4	12.8
December-2009	HR	M-19	5	0.8	8.3	9.1	0.09	0.13	0.62	0.43	0.41	7.1	7.7	17.1	20.2	11.3
		M-20	25	0.1	0.6	0.7	0.09	0.16	0.65	0.37	0.40	7.1	7.7	17.1	21.9	8.4
	CR	M-21	5	0.3	3.3	3.6	0.10	0.13	0.59	0.51	0.41	7.1	7.7	17.3	18.6	15.3
		M-22	25	0.4	5.0	5.4	0.08	0.11	0.61	0.52	0.39	7.1	7.7	17.3	19.7	16.2
	BCD	M-23	5	1.4	7.6	9.0	0.19	0.20	0.48	0.52	0.42	6.6	7.7	17.0	12.5	15.8
		M-24	15	1.2	16.1	17.3	0.07	0.09	0.45	0.50	0.40	7.1	7.7	17.2	10.8	15.1
	BAD	M-25	4	7.1	8.1	15.2	0.87	0.57	0.49	0.67	0.44	6.9	7.6	16.9	13.0	23.5
		M-26	5	0.2	2.7	3.0	0.09	0.11	0.45	0.52	0.41	6.9	7.7	17.1	10.8	16.1
		M-27	25	0.4	4.5	4.9	0.08	0.11	0.51	0.45	0.40	6.9	7.7	17.1	14.2	12.8
June-2010	Above the dam	S-1	0.2	17.4[c]	3.4[c]	20.8[c]	5.04	0.92	0.74	0.91	0.71	6.1	6.9	30.2	26.8	32.9
	BCD	S-2	0.2	355.2[c]	71.2[c]	426.4[c]	4.99	0.91	0.79	0.68	0.22	5.9	8.2	31.0	29.6	25.7
	Close to BCD	S-3	0.2	10.9[c]	1.7[c]	10.12[c]	5.01	0.91	1.00	0.83	0.81	6.0	6.6	32.0	41.2	28.1

[a] Letianxi Stream.
[b] Letianxi Stream mouth to the Yangtze River.
[c] In ng/g.

(9/1, v/v). GDGTs were analyzed using single ion monitoring (SIM) of m/z 1302, 1300, 1298, 1296, 1292, 1050, 1048, 1046, 1036, 1034, 1032, 1022, 1020 and 1018. The conditions for the ion source were: nebulizer pressure 40 psi, vaporizer temperature 350 °C, drying gas (N_2) 5 l/min, temperature 250 °C, capillary voltage 3 kV and corona 4 μA. Quantification was performed via peak area integration of the $[M+1]^+$ ions.

Cluster analysis of individual *i*GDGTs or *b*GDGTs normalized to the sum of each lipid pool was performed using Cluster analysis software R-2.12.1 based on the squared Euclidean distance using the method of two-way jointing.

TEX_{86} and river water temperature were calculated according to Schouten et al. (2002) and Powers et al. (2010), respectively:

$$\mathrm{TEX}_{86} = [\mathrm{VII} + \mathrm{VIII} + \mathrm{IV}']/[\mathrm{VI} + \mathrm{VII} + \mathrm{VIII} + \mathrm{IV}'] \quad (1)$$

$$T = -14.0 + 55.2 \times \mathrm{TEX}_{86} \quad (2)$$

MBT, CBT and derived annual mean air temperature or soil pH were calculated according to Weijers et al. (2007b):

$$\mathrm{MBT} = [\mathrm{I} + \mathrm{Ib} + \mathrm{Ic}]/[\mathrm{I} + \mathrm{Ib} + \mathrm{Ic} + \mathrm{II} + \mathrm{IIb} + \mathrm{IIc} + \mathrm{III} + \mathrm{IIIb} + \mathrm{IIIc}] \quad (3)$$

$$\mathrm{CBT} = -\log[(\mathrm{Ib} + \mathrm{IIb})/(\mathrm{I} + \mathrm{II})] \quad (4)$$

$$T_{\mathrm{MBT/CBT}} = (\mathrm{MBT} - 0.122 - 0.187 \times \mathrm{CBT})/0.02 \quad (5)$$

$$\mathrm{pH}_{\mathrm{CBT}} = (3.33 - \mathrm{CBT})/0.38 \quad (6)$$

BIT was calculated according to Hopmans et al. (2004):

$$\mathrm{BIT} = [(\mathrm{I} + \mathrm{II} + \mathrm{III})/(\mathrm{I} + \mathrm{II} + \mathrm{III} + \mathrm{IV})] \quad (7)$$

The recent calibration of MBT–CBT proxies by Peterse et al. (2012) was also applied, but found to afford similar temperature estimates.

3. Results

3.1. Abundance and distribution of GDGTs above and below TGD

The abundance of *i*GDGTs and *b*GDGTs in the SPM varied seasonally and by location (Table 1). They were in low abundance in samples from a tributary river or not detected in one of the HR samples in July, 2009 (Table 1). Overall, the profiles in the SPM samples along the TGD in the Yangtze River showed a predominance of bacterial *b*GDGTs over archaeal *i*GDGTs in May and July of 2009, respectively; however, the concentration of archaeal *i*GDGTs increased considerably in December (Table 1). This was also demonstrated from the BIT index, which was > 0.8 in May and July but < 0.2 in December (Table 1). The concentration of *i*GDGTs ranged from 0.1–16.1 ng/l for SPM samples, with relatively higher values primarily in the winter season (Table 1). Among the *i*GDGTs, crenarchaeol accounted for 35.2% on average and GDGT-0 for 39.5%. GDGT-VI, -VII -VIII and –VI′ were detected in most samples, with much lower concentration in most surface SPM samples (Supplementary Table 1). On the other hand, total *b*GDGTs were present in very low amount in December (average 13.0% of total GDGTs) when the water flow was low. One exception was M-25 (SPM sample from BAD collected in December, 2009) that had a *b*GDGTs abundance of 46.5%. Of all the *b*GDGTs, GDGT I and GDGT II were the most abundant (average 29.7% and 35.1%, respectively) in different seasons, followed by GDGT III (12.0% on average; Supplementary Table 2).

A ternary diagram shows the relative abundance of crenarchaeol (IV), GDGT-0 (V), and sum of *b*GDGTs (I + II + III) (three major groups; Fig. 3). Overall, crenarchaeol was the dominant individual *i*GDGT in December (relative abundance > 62.7% in three major groups) and was found in relatively small amount in May and July, varying from 6.5% to 39.5% of the three major GDGTs (Fig. 3). GDGT-0 in most SPM samples ranged between 9.1% and 26.9% of the three major groups in May and July, respectively, but slightly increased to 14.3–31.2% in December (Table 2).

In the soil samples, the *b*GDGTs were predominant, with a relative abundance of > 88.8% of the three components; whereas crenarchaeol and GDGT-0 were below 8.6% and 2.6%, respectively (Table 2). Total GDGTs from Letianxi Stream were 2.7 ng/l in July (M-16) and 0.9 ng/l in May (M-7), which was either higher (May) or lower (July) than those from the main channel of the Yangtze below the dam (Fig. 2; Table 1).

The GDGTs in the SPM also varied with depth above the dam. During the flooding season, the *b*GDGTs in SPM from relatively deep levels (15 m or 25 m) were more abundant than in SPM from the near surface (5 m) (Table 1). The total GDGT concentration along the channel was similar in December and May of 2009, but GDGTs were in substantially higher amount below the TGD than above the TGD in July, 2009 (Table 1).

The overall spatial GDGT distribution patterns for various samples collected in different seasons are shown in Fig. 5 using cluster

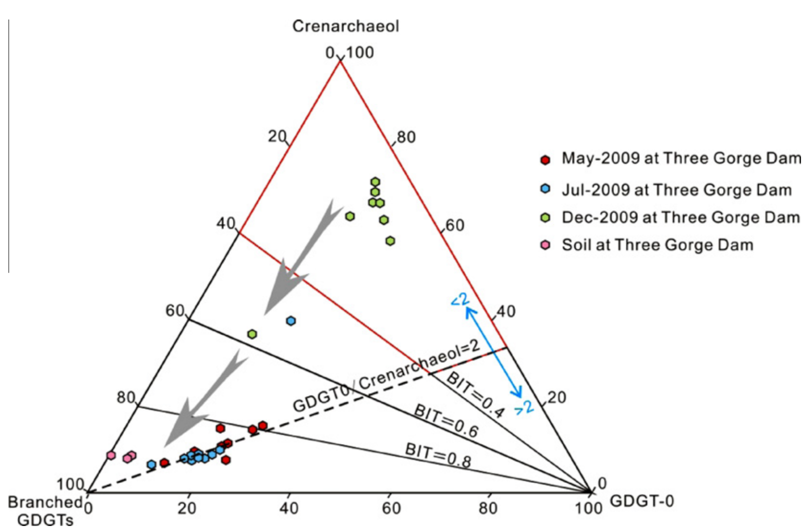

Fig. 3. Ternary diagram indicating composition of major GDGTs in suspended particulate matter and soil collected in May, July and December, respectively.

analysis. In general, *i*GDGTs (Fig. 4a) were separated by season whereas *b*GDGTs (Fig. 4b) were not. In both cases, however, the soil samples were distinct from the river samples (Fig. 4a and b).

3.2. Calculation of GDGT-derived proxies above and below TGD

The TEX_{86} values for SPM samples correlated significantly with measured river surface temperature (RST) (Figs. 5 and 6a; R^2 0.55, $P = 0.00004$, $n = 27$). When grouped by sampling season, TEX_{86} derived temperature more or less reflected the average river water temperature measured for that month at different depths (Fig. 5); the weighted average TEX_{86} temperature was 16.6 ± 4.1 °C in December and about 0.5 °C lower than the measured temperature (17.1 °C), 22.2 ± 2.8 °C in May and about 1.4 °C higher than the measured temperature (20.8 °C), and 24.8 ± 1.8 °C in July, 2.1 °C lower than the measured temperature (26.9 °C; Fig. 6d).

The CBT index from water and soil varied between 0.22 and 0.81 and the MBT index between 0.37 and 0.91; the two indices correlated significantly (R^2 0.48, $P = 0.017$, $n = 27$; Fig. 6b). When the MBT/CBT-derived temperature was plotted vs. measured water temperature, no significant correlation was observed; instead, the MBT/CBT-calculated monthly average temperature (14.9 ± 1.3 °C for December, 16.2 ± 1.4 °C for May, 14.6 ± 1.1 °C for July) values were all closer to the annual mean air temperature (16.9 °C) than to the monthly mean air temperature in each season (Fig. 6e).

The CBT values for SPM showed a poor correlation with measured pH (Fig. 6c) and the CBT-calculated pH (7.4–8.0) generally underestimated the actual pH of the river water in May–July and overestimated it in December (Fig. 6f). The soil samples had CBT values ranging from 0.22 to 0.81 (Fig. 6c), which corresponded to CBT-derived pH of around 6.6–8.2. These values were slightly higher than the measured soil pH (6.0; Fig. 6f, Table 1).

4. Discussion

4.1. Factors controlling distribution of iGDGTs in river water

Numerous studies have reported that crenarchaeol in various settings can originate from a unique group of *Thaumarchaeota* (Schouten et al., 2000; Sinninghe Damsté et al., 2000; Pearson et al., 2004; Powers et al., 2004, 2010; Weijers et al., 2004, 2006b; Zhang et al., 2006; Herfort et al., 2009). It has a higher concentration in marine, lacustrine environments and peat bogs than in soil (Weijers et al., 2006b). Studies have indicated that high pH is an important factor leading to high *i*GDGT/*b*GDGT ratio values and consequently lower BIT values in soil, with a high abundance of *i*GDGTs being generally found in an alkaline environment (Weijers et al., 2006b, 2007b; Lauber et al., 2009; Huguet et al., 2010; Peterse et al., 2010; Yang et al., 2012).

In this study, the riverine system in different seasons is just below neutral to slightly alkaline, with pH ranging from 6.6 to 8.3, as compared with the slightly acidic environments (pH 5.9–6.1) for surface soil along the TGD (Table 1). Hence, it seems likely that aquatic production of crenarchaeol may not potentially affect pH values in the TGD. In particular, the BIT value in SPM is significantly correlated with *i*GDGT concentrations (R^2 0.72, $P = 0.000001$, $n = 17$) but, to a lesser degree, with *b*GDGT components (R^2 0.07, $P = 0.06$, $n = 17$) in the flooding season (May and July). In contrast, the correlation between BIT values of SPM and *b*GDGT concentration increases significantly (R^2 0.94, $P = 0.006$, $n = 9$) in winter, but shows relatively low correlation with *i*GDGTs during winter (R^2 0.01, $P = 0.18$, $n = 9$). This would indicate that the BIT variation primarily reflects change in riverine crenarchaeol production rather than soil-derived *b*GDGT flux in summer, and vice versa. Similar conclusions have been made in studies of the Congo Fan (Weijers et al., 2009), African lakes (Tierney et al., 2010) and lower River Amazon (Kim et al., 2012). In this study, however, the precipitation is high in summer (ca. 130 mm in May and ca. 220 mm in July), which might have enhanced the soil erosion and caused an important supply of terrestrial GDGTs to the river (Fig. 4a). Besides, the higher input of groundwater to the Yangtze River water (ca. 20–30%; Shi et al., 2002; Chen and Saito, 2011) and increasing accelerated anthropogenic activity (Wang et al., 2008; Xu and Milliman, 2009), such as sequestration of upstream sediments by the dams, stagnation and eutrophication of reservoirs, might also impact the production of GDGTs. In contrast, the high crenarchaeol concentration relative to *b*GDGT pool in December may be derived from *Thaumarchaeota* living in the river or the reservoir above the dam due to water stagnation (Herfort et al., 2009; Blaga et al., 2011). We therefore compared the GDGT concentration between a lake (Blaga et al., 2011) and the TGD area, which did show very similar patterns in GDGT concentration in the SPM. Concentration of *i*GDGTs increased with depth, with maximum values in the deeper part of the water column. This indicated production of *i*GDGTs by *Thaumarchaeota* in the deep water. However, crenarchaeol from soil erosion may also contribute to its abundance in the river/reservoir during winter season, although this contribution might be small.

GDGT-0 is most likely produced by methanogens as well as *Thaumarchaeota* (Schouten et al., 2002; Weijers et al., 2006b; Blaga et al., 2009). A GDGT-0/crenarchaeol ratio between 0.2 and 2 indicates *Thaumarchaeota* as a source, while a value > 2 indicates a source from methanogens or other Euryarchaeota (Schouten et al., 2002; Blaga et al., 2009; Sinninghe Damsté et al., 2009; Fig. 3). Most of the December samples had an average GDGT-0/crenarchaeol value < 0.4, indicating that all SPM samples probably had a primary source of *Thaumarchaeota*. The ratio in May was, however, much higher, varying from 1.25 to 1.96 (Fig. 3; Table 2). The ratio of GDGT-0/crenarchaeol for M-4 (25 m depth) even increased to 3.15, likely from in situ production of methanogen biomass or imported soil-derived methanogens just above the TGD. Other studies have already indicated that methanogens and other *Euryarchaeota* and *Thaumarchaeota* are the most likely sources for GDGT-0 in lacustrine environments (Sinninghe Damsté et al., 2002, 2012; Weijers et al., 2006b; Blaga et al., 2009; Pearson et al., 2011). Our results can thus be explained by mixed soil derived/aquatic *Euryarchaeota* for the GDGTs above the dam due to water stagnation. During the flooding season, the ratio of GDGT-0/crenarchaeol for SPM collected in July of 2009 primarily concentrated along the line of GDGT-0/crenarchaeol equal to 2 (Fig. 3). It is possible that this value reflects the contribution of soil-derived methanogens and other *Archaea* (Blaga et al., 2009). One exception is sample M-15 from 15 m, which had a GDGT-0/crenarchaeol value of 0.52, indicating a substantial input of *Thaumarchaeota* relative to those of methanogenic GDGTs in the mid-depth water, possibly due to re-suspension of oxic sediment in the shallow river, which contains mainly *Thaumarchaeota*. Since a wide range of organisms in the archaeal domain can biosynthesize GDGT-0 (Schouten et al., 2007), the sources of GDGT-0 in the surface river water may be more complicated than described here. No significant increase in GDGT-0 with water depth was noted in the flooding season, though the relatively high ratio of GDGT-0/crenarchaeol (> 2) in the middle water occurred just above the TGD (M-12 and M-13 at HR; Table 2). Intriguingly, there was also disparity in the ratio of *b*GDGTs/*i*GDGTs at different depths between CR and BCD over the year, with a small difference below the dam and a large difference emerging after the dam (Table 1), suggesting intense mixing of the water at deeper depth at locations above the TGD (Fig. 5). It is thus anticipated that the *b*GDGTs/*i*GDGTs ratio in the TGD area, where the BIT values are high and terrestrial input is distinct, would reflect the partial, if not whole, impact of TGD on the composition of the archaeal population in each season.

Table 2
Relative abundance (% of total) of GDGTs and BIT and GDGT-0/crenarchaeol values for SPM in the Yangtze River and soil along the TGD.

Season	Location	Point	Depth (m)	Relative abundance[a] (%)			BIT	GDGT-0/crenarchaeol	GDGT-2%/(VII/(VI + VII + VIII + Cren′) × 100
				GDGT-0	Crenarchaeol	*b*GDGTs			
May-2009	HR	M-1	5	21.1	10.8	68.2	0.86	1.96	23.80
		M-2	25	11.8	7.0	81.2	0.92	1.69	27.01
	CR	M-3	5	26.9	15.6	57.5	0.79	1.72	25.78
		M-4	25	23.7	7.5	68.8	0.90	3.15	28.34
	BCD	M-5	5	25.3	14.7	60.0	0.80	1.72	30.09
		M-6	5	16.2	9.8	74.0	0.88	1.65	28.48
	BAD	M-7	2.5	18.9	15.1	66.1	0.81	1.25	33.54
		M-8	5	22.1	11.5	66.3	0.85	1.92	24.30
July-2009	HR	M-9	5	17.8	8.0	74.2	0.90	2.24	30.31
		M-10	25	15.1	7.9	77.0	0.91	1.90	30.27
	CR	M-11	5	16.0	8.6	75.4	0.90	1.86	17.94
		M-12	15	20.2	8.7	71.0	0.89	2.32	24.14
		M-13	25	21.1	10.1	68.8	0.87	2.08	38.87
	BCD	M-14	5	16.6	7.4	76.0	0.91	2.26	29.79
		M-15	15	20.6	39.5	39.9	0.50	0.52	35.13
		M-16	3	9.1	6.5	84.3	0.93	1.39	42.41
	BAD	M-17	5	17.2	8.9	73.9	0.89	1.94	28.62
		M-18	5	19.2	8.0	72.8	0.90	2.40	28.01
December-2009	HR	M-19	5	27.4	62.9	9.7	0.13	0.44	25.22
		M-20	25	31.2	57.9	10.9	0.16	0.54	22.00
	CR	M-21	5	23.2	66.9	10.0	0.13	0.35	30.36
		M-22	25	24.9	66.5	8.6	0.11	0.37	27.87
	BCD	M-23	5	20.1	63.7	16.3	0.20	0.31	36.23
		M-24	15	21.3	71.6	7.1	0.09	0.30	35.55
		M-25	4	14.3	36.5	49.2	0.57	0.39	36.40
	BAD	M-26	5	21.9	69.3	8.9	0.11	0.32	35.60
		M-27	25	22.6	69.2	8.2	0.11	0.33	33.02
June-2010	Above the dam	S-1	0.2	3.8	8.1	88.1	0.92	0.47	31.92
	BCD	S-2	0.2	4.0	8.7	87.3	0.91	0.46	51.95
	Close to BCD	S-3	0.2	0.0	8.9	91.1	0.91	0.00	0.00

[a] Sum of GDGT-0, crenarcheol and *b*GDGTs (I + II + III) is 100%.

4.2. Factors constraining the distribution of bGDGTs

The *b*GDGTs I–III were the most abundant components in all SPM samples in May and July but became less important in December (Fig. 4b; Tables 1 and 2). A high abundance of *b*GDGTs is generally found in acidic environments (Weijers et al., 2006b, 2007b; Lauber et al., 2009; Huguet et al., 2010; Peterse et al., 2010), suggesting the possibility of *b*GDGT generation from the *Acidobacteria* phylum (Weijers et al., 2009; Peterse et al., 2010; Sinninghe Damsté et al., 2011). Thus the measured pH values (7.1–8.3) in the Yangtze River may not be favorable for organisms producing *b*GDGTs. This implies that *b*GDGTs in the aquatic environment are partially soil-derived through runoff, particularly in summer (May and July). This is supported by a comparatively higher concentration of *b*GDGTs in July (average 4.8 ng/l) or higher ratio of *b*GDGTs/*i*GDGTs in summer (2.6 on average), as well as a higher BIT index over the flooding season (0.85 in May and 0.86 in July, respectively; Tables 1 and 2). However, the pronounced maximum in *b*GDGTs in the water column, especially in the deeper water during the flooding season, may also represent in situ production or transport by groundwater entering the river. Indeed, studies of several lakes have suggested that the in situ production of *b*GDGTs is probable (Sinninghe Damsté et al., 2009, 2012; Blaga et al., 2010; Zink et al., 2010; Sun et al., 2011; Kim et al., 2012). In addition, ca. 20–30% of annual water inflow to the river is groundwater (Yao et al., 2007; Zhu et al., 2011) and percolates through well-developed soils of the upper montane forest. Further information on the provenance of the *b*GDGTs in the river can be obtained by comparing their distributions, as expressed by MBT and CBT. A cross plot of these two parameters (Fig. 6b) shows wide variation in the *b*GDGT composition of the soil. In comparison, the distribution of *b*GDGTs in particles setting through the year is relatively uniform, with MBT values ranging from 0.4 to 0.6 and CBT between 0.3 and 0.5. These results suggest that it is unlikely that rainfall leached significant amounts of *b*GDGTs from soils and transported them to the river, in agreement with studies of the River Amazon (Bendle et al., 2010; Kim et al., 2012).

Our water column data also revealed that both the *b*GDGT distribution and ratio of *b*GDGTs/*i*GDGTs in December were substantially lower than those in summer, with *b*GDGT input only accounting for 18% of *i*GDGTs (Table 1). One viable explanation for this decreased *b*GDGT concentration relative to increased *i*GDGT source might be the aquatic production in the riverine system.

The exact soil source of river *b*GDGTs at the TGD is unknown; the majority are likely from upstream of the river. The major tributaries at the TGD might also contribute to the *b*GDGT pool at the dam; however, because the Letianxi Stream is a very small tributary (contributing <10% of water flow to the main Yangtze channel), its impact on the main stream GDGTs may be small.

4.3. TEX_{86} palaeothermometry

Studies have indicated that TEX_{86} palaeothermometry is only applicable if the source of the GDGTs is *Thaumarchaeota* and the BIT index is < 0.4 (Schouten et al., 2002; Pancost and Sinninghe Damsté, 2003; Weijers et al., 2006b; Blaga et al., 2009; Powers et al., 2010). In this study, even though the BIT had a wide range from 0.09 to 0.93, the overall TEX_{86} derived temperature reflected the in situ river temperature (Table 1). Although the TGD area is dominated by a subtropical monsoon climate with an annual average precipitation of 1200 mm (Chen et al., 2001; Jiang, 2007), the ratio of *b*GDGTs to *i*GDGTs (and the BIT value) for three soil samples changed little (ranging from 4.99 to 5.04; Table 1). However, variation in this ratio in the water column seems dependent on

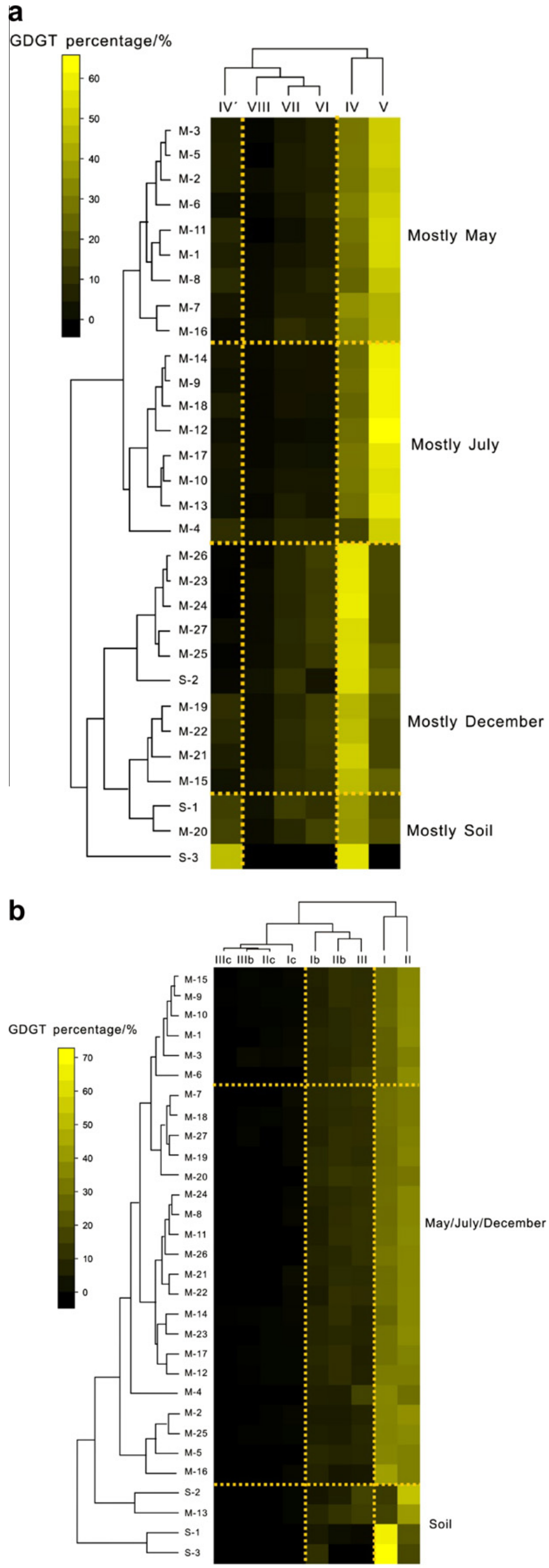

Fig. 4. Cluster analysis showing temporal–spatial distribution of *i*GDGTs (a) and *b*GDGTs (b).

the seasonal settings (average 2.2, 3.0 and 0.18 in May, July and December, respectively), suggesting an overall higher soil-derived contribution of *i*GDGTs (52%) in summer and extremely lower contribution (4%) in winter.

Although individual data are scattered and deviate from surface temperature, TEX_{86} derived temperatures overall reflect the average river water temperature measured for that month (Fig. 6d). One way of judging whether GDGT distributions are suitable for TEX_{86} palaeothermometry involves examination of GDGT-0/crenarchaeol (Blaga et al., 2009) and GDGT-2% values ([VII/(VI + VII + VIII + Cren′) × 100]; Sinninghe Damsté et al., 2012), based on the fact that for enrichment cultures of *Thaumarchaeota* the two ratios are always < 2% and < 45%, respectively (Blaga et al., 2009; Sinninghe Damsté et al., 2012). In this study, GDGT-0/crenarchaeol and GDGT-2% for most SPM and soils had average values of 1.3 and 29.8, respectively, consistent with their dominant source being the pelagic *Thaumarchaeota* (Table 2). It is thus reasonable to argue that TEX_{86} values for most samples are suitable for TXE_{86} palaeothermometry in this riverine system near the TGD.

Given the analytical uncertainty in RST (4.1 °C), our reconstructed RST values do not deviate from measured actual river temperature values (average < 2.1 °C and almost within the calibration error), implying the robustness of the TEX_{86} RST in TGD and potentially in similar environments. Besides, our results are in good agreement with observations for low latitude lakes (Powers et al., 2005; Sinninghe Damsté et al., 2012) and the North Sea (Wuchter et al., 2005, 2006). Therefore, the fidelity of TEX_{86} values in the river water at the TGD may not be limited to a BIT index of < 0.4 (Fig. 6d); however, it needs to be verified as to whether or not this applies to other freshwater systems similar to the Yangtze River.

Our results, together with those from other studies (Weijers et al., 2006b; Blaga et al., 2009; Kim et al., 2010; Yang et al., 2012), show that in some of the SPM samples GDGTs were synthesized by *Thaumarchaeota*, which allowed for TEX_{86} temperature reconstruction in the freshwater system. The large scatter for the SPM samples using the TEX_{86} calibration requires detailed investigation of the ecology of *Thaumarchaeota* in such a large river to further understand how seasonal climatic change and water depth affect the relative abundance of the GDGTs in such a river system.

4.4. Estimation of air temperature and soil pH using bGDGTs

Weijers et al. (2007a) used the soil-based MBT/CBT calibration to successfully construct mean annual air temperature (MAAT) and soil pH [Eqs. (5) and (6), respectively]. The average CBT/MBT-derived temperature for the *b*GDGTs in the SPM (15.2 ± 0.7 °C) is close to the MAAT (16.9 °C) in the sampling region, highlighting the potential of MBT/CBT proxies for annual average temperature in a big river system. In addition, the high sedimentation rate (Yao et al., 2007) also enabled the MBT/CBT-calculated temperature to offer a more accurate estimating of the local signal.

The MBT/CBT derived MAAT estimates based on the *b*GDGT distributions in the soil samples varied between 25.7 and 32.9 °C (Table 1); the upper values are close to the measured in situ surface soil temperature in June (Table 1). It is unclear whether or not this indicates a response of soil *b*GDGTs to seasonal temperature variation. Weijers et al. (2011) observed no seasonal temperature effect on *b*GDGTs for mid-latitude soils. More soil samples need to be collected in different seasons to verify whether or not this is the case in the Yangtze River drainage basin.

The CBT pH index for SPM likely represents the catchment condition rather than the local signal. This is because of partial allochthonous terrestrial input of soil-derived GDGTs that may be enhanced by the intensive anthropogenic activity, high precipitation and large groundwater influx (as shown in higher BIT values, especially in summer season). Subsequently, our study results in

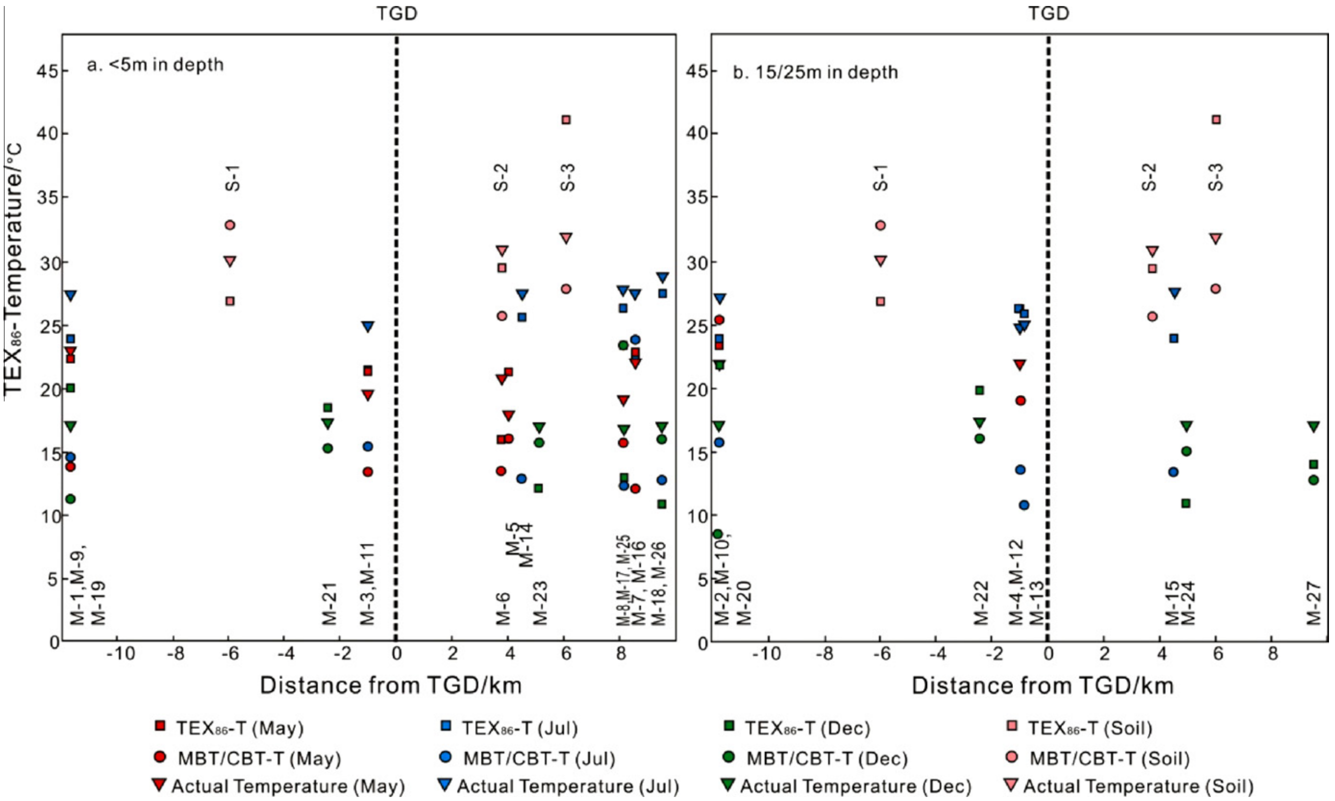

Fig. 5. Spatial variation in compounds, showing distribution of TEX_{86} derived temperature for samples in the TGD area at different depths: (a) < 5 m; (b) 15 or 25 m.

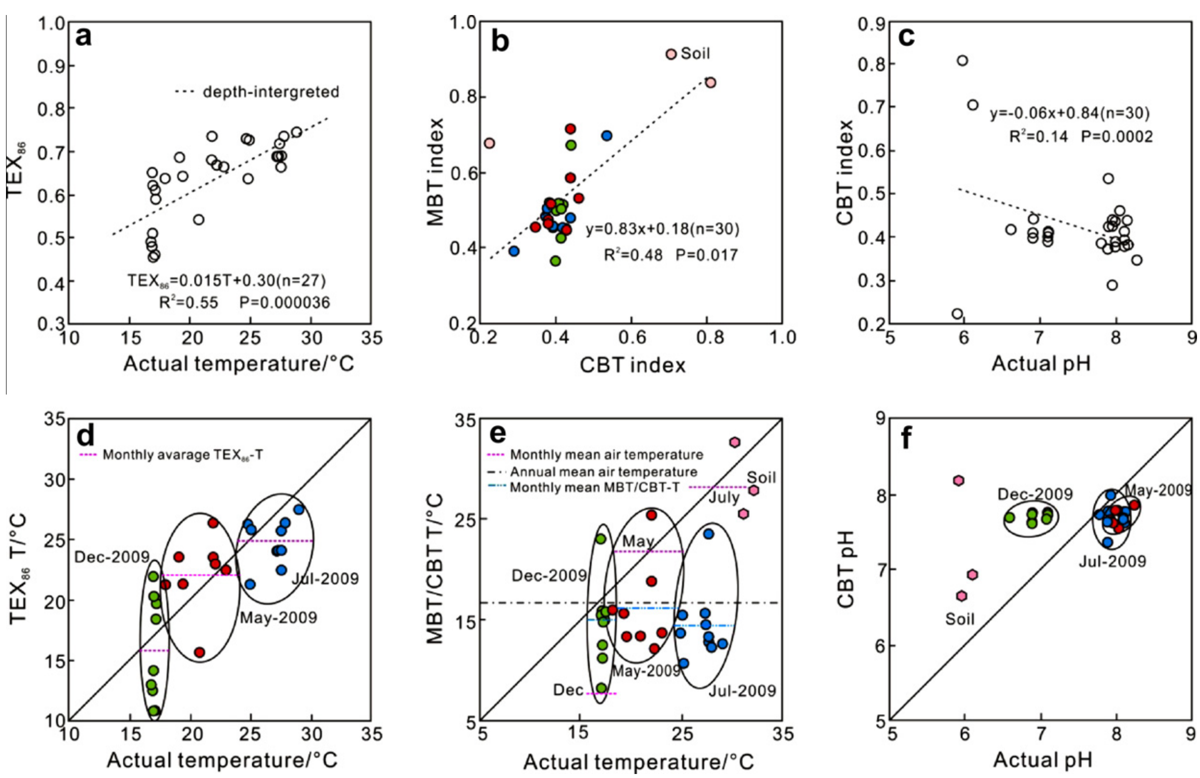

Fig. 6. Biplots showing variation in TEX_{86}, MBT or CBT as a function of measured water temperature (a) and pH (c), and correlation between MBT–CBT values (b), TEX_{86}-derived temperature and measured water temperature (d), CBT/MBT-derived temperature and measured soil temperature (e) and CBT-derived pH and measured pH (f). The diagonal lines in d, e, and f are the 1:1 ratio line.

an average pH of 7.7 ± 0.6 in SPM, almost identical to the measured pH (7.7 on average). We speculate that the variation in soil erosion and riverine compound reactivity with season might slightly underestimate/overestimate the actual pH of the river water in summer/winter. However, our CBT-reconstructed pH value for soil samples shows a large variation ranging from 6.6 to 8.2 and is slightly higher than the measured soil pH (6.0; Fig. 6f, Table 1), likely suggesting in situ production of branched GDGTs along the flanks of the Yangtze River. In such settings, a local calibration is necessary and the ecological niches of bacteria producing *b*GDGTs along the TGD from the Yangtze River need to be clearly defined before definitive conclusions can be made. We also know little about the reservoir effect near the TGD, which may alter the terrestrial input to the water from season to season.

The results between MBT/CBT-derived temperature and CBT derived pH suggest that the sources of *b*GDGTs in the river water are complicated and might not be solely derived from local soil runoff. Further investigations are necessary to study how changes in the distribution of *b*GDGTs respond to environmental variations in such systems.

5. Conclusions

Our study shows that *i*GDGTs derived from *Thaumarchaeota* are abundant near the TGD in the Yangtze River. Despite being integrated over a large segment of the Yangtze, the TEX_{86} proxy appears to reflect the local river water temperature in different seasons of the year. However, changes in precipitation, soil runoff and the extent of stagnation of water above the TGD may be the reason for the wide variation in TEX_{86} values. The consistency between average CBT/MBT derived temperature for the SPM (15.2 ± 0.7 °C) and the annual mean air temperature (16.9 °C) led to the conclusion that the MBT/CBT indices for the SPM samples likely reflect the annual average air temperature instead of seasonal variation. The results expand the application of MBT/CBT and TEX_{86} proxies for climate studies of riverine systems.

Acknowledgements

We thank J.X. Wang for support with LC–MS analysis and C. Warren for improving the English in the paper. We thank the anonymous reviewers for constructive comments and suggestions. The research is partially supported by the National Natural Science Foundation of China No. 41002036 (G.F.Y.) and No. 91028005 (C.L.Z.), the Fundamental Research Funds for the Central Universities (G.F.Y.; No. 2011YYL129), the National "1000 Talents Program" (C.L.Z.) and the State Key Laboratory of Marine Geology at Tongji University (No. MGK1002), and the Biogeology and Environmental Geology at China University of Geosciences (No. BGEG201102).

Appendix A. Supplementary material

Supplementary data associated with this article can be found, in the online version, at http://dx.doi.org/10.1016/j.orggeochem.2012.11.014.

Associate Editor—**S. Schouten**

References

Bendle, J.A., Pancost, R.D., Weijers, J.W., Maslin, M.A., Sinninghe Damsté, J.S., Schouten, S., Hopmans, E.C., Boot, C., 2010. Major changes in Last Glacial and Holocene terrestrial temperatures and sources of organic carbon recorded in the Amazon fan by the MBT/CBT continental paleothermometer. Geochemistry, Geophysics and Geosystems (G-cubed) 11, Q12007. http://dx.doi.org/10.1029/2010GC003308.

Blaga, C.I., Reichart, G.J., Heiri, O., Sinninghe Damsté, J.S., 2009. Tetrather membrane lipid distributions in lake particulate matter and sediments: a study of 47 European lakes along a North–South transect. Journal of Paleolimnology 41, 523–540.

Blaga, C.I., Reichart, G.J., Schouten, S., Lotter, A.F., Werne, J.P., Kosten, S., Mazzeo, N., Lacerot, G., Sinninghe Damsté, J.S., 2010. Branched glycerol dialkyl glycerol tetraethers in lake sediments: can they be used as temperature and pH proxies? Organic Geochemistry 41, 1225–1234.

Blaga, C.I., Reichart, G.-J., Vissers, E.W., Lotter, A.F., Anselmetti, F.S., Sinninghe Damsté, J.S., 2011. Seasonal changes in glycerol dialkyl glycerol tetraether concentrations and fluxes in a perialpine lake: implications for the use of the TEX_{86} and BIT proxies. Geochimica et Cosmochimica Acta 75, 6416–6428.

Brochier-Armanet, C., Boussau, B., Gribaldo, S., Forterre, P., 2008. Mesophilic crenarchaeota: proposal for a third archaeal phylum, the Thaumarchaeota. Nature Reviews 6, 245–252.

Chen, Z., Saito Y. (Eds.), 2011. The mega-deltas of Asia: interlinkage of land and sea and human development. Earth Surface Processes and Landforms 36. doi: http://dx.doi.org/10.1002/esp.2190.

Chen, Z., Yu, L.Z., Gupta, A. (Eds.), 2001. Yangtze River, China. Geomorphology 41 (special issue), pp. 1–248.

Colloschonn, W., Tucci, C.E.M., Clarke, R.T., 2001. Further evidence of changes in the hyrological regime of the River Paraguay: part of a wider phenomenon of climate changes? Journal of Hydrology 245, 218–238.

DeLong, E.F., 1998. Everything in moderation: Archaea as "non-extremophiles". Current Opinion in Genetics & Development 8, 649–654.

Herfort, L., Schouten, S., Boon, J.P., Woltering, M., Baas, M., Weijers, J.W.H., 2006. Characterization of transport and deposition of terrestrial organic matter in the southern North Sea using the BIT index. Limnology and Oceanography 51, 2196–2205.

Herfort, L., Kim, J.-H., Coolen, M.J.L., Abbas, B., Schouten, S., Hernal, G.J., Sinninghe Damsté, J.S., 2009. Diversity of Archaea and potential for crenarchaeotal nitrification of group 1.1a in the rivers Rhine and Têt. Aquatic Microbial Ecology 55, 189–201.

Hopmans, E.C., Weijers, J.W.H., Schefuß, E., Herfort, L., Sinninghe Damsté, J.S., Schouten, S., 2004. A novel proxy for terrestrial organic matter in sediments based on branched and isoprenoid tetraether lipids. Earth and Planetary Science Letters 224, 107–116.

Huguet, C., Hopmans, E.C., Febo-Ayala, W., Thompson, D.H., Sinninghe Damsté, J.S., Schouten, S., 2006. An improved method to determine the absolute abundance of glycerol dibiphytanyl glycerol tetraether lipids. Organic Geochemistry 37, 1036–1041.

Huguet, A., Fosse, C., Metzger, P., Fritsch, E., Derenne, S., 2010. Occurrence and distribution of extractable glycerol dialkyl glycerol tetraethers in podzols. Organic Geochemistry 41, 291–301.

Jiang, H.R., 2007. China Meteorological Disasters: Hubei Province. Beijing, China Meteorological Press, pp. 1–462 (in Chinese).

Kim, J.-H., Ludwig, W., Schouten, S., Kerhervé, P., Herfort, L., Bonnin, J., Sinninghe Damsté, J.S., 2007. Impact of flood events on the transport of terrestrial organic matter to the ocean: a study of the Têt River (SW France) using the BIT index. Organic Geochemistry 38, 1593–1606.

Kim, J.-H., Schouten, S., Hopmans, E.C., Donner, B., Sinninghe Damsté, J.S., 2008. Global sediment core-top calibration of the TEX_{86} paleothermometer in the ocean. Geochimica et Cosmochimica Acta 72, 1154–1173.

Kim, J.-H., Zarzycka, B., Buscail, R., Peterse, F., Bonnin, J., Ludwig, W., Schouten, S., Sinninghe Damsté, J.S., 2010. Contribution of river-borne soil organic carbon to the Gulf of Lions (NW Mediterranean). Limnology and Oceanography 55, 507–518.

Kim, J.-H., Zell, C., Moreira-Turcq, P., Pérez, M.A.P., Abril, G., Mortillaro, J.-M., Weijers, J.W.H., Meziane, T., Sinninghe Damsté, J.S., 2012. Tracing soil organic carbon in the lower Amazon River and its tributaries using GDGT distributions and bulk organic matter properties. Geochimica et Cosmochimica Acta 90, 163–180.

Lauber, C.L., Hamady, M., Knight, R., Fierer, N., 2009. Pyrosequencing-based assessment of soil pH as a predictor of soil bacterial community structure at the continental scale. Applied and Environment Microbiology 75, 5111–5120.

Ménot, G., Bard, E., Rostek, F., Weijers, J.W.H., Hopmans, E.C., Schouten, S., Sinninghe Damsté, J.S., 2006. Early reactivation of European rivers during the last deglaciation. Science 313, 1623–1625.

Meyers, P.A., 1994. Preservation of elemental and isotopic source identification of sedimentary organic matter. Chemical Geology 114, 289–302.

Milliman, J.D., Syvitski, J.P.M., 1992. Geomorphic/tectonic control of sediment discharge to the ocean: the importance of small mountainous rivers. Journal of Geology 100, 525–544.

Millman, J.D., Meade, R.H., 1983. World-wide delivery of sediment to the oceans. Journal of Geology 91, 1–21.

Pancost, R.D., Sinninghe Damsté, J.S., 2003. Carbon isotopic compositions of prokaryotic lipids as tracers of carbon cycling in diverse settings. Chemical Geology 1195, 29–58.

Pancost, R.D., Van Geel, B., Baas, M., Sinninghe Damsté, J.S., 2000. $\delta^{13}C$ values and radiocarbon dates of microbial biomarkers as tracers for carbon recycling in peat deposits. Geology 28, 663–666.

Pearson, A., Huang, Z., Ingalls, A.E., Romanek, C.S., Wiegel, J., Freeman, K.H., Smittenberg, R.H., Zhang, C.L., 2004. Nonmarine crenarchaeol in Nevada hot springs. Applied and Environmental Microbiology 70, 5229–5237.

Pearson, E.J., Juggins, S., Talbot, H.M., Weckström, J., Rosén, P., Ryves, D.B., Roberts, S.J., Schmidt, R., 2011. A lacustrine GDGT-temperature calibration from the Scandinavian Arctic to Antarctic: renewed potential for the application of GDGT-paleothermometry in lakes. Geochimica et Cosmochimica Acta 75, 6225–6238.

Pester, M., Schleper, C., Wagner, M., 2011. The Thaumarchaeota: an emerging view of their phylogeny and ecophysiology. Current Opinion in Microbiology 14, 300–306.

Peterse, F., Nicol, G.W., Schouten, S., Sinninghe Damsté, J.S., 2010. Influence of soil pH on the abundance and distribution of core and intact polar lipid-derived branched GDGTs in soil. Organic Geochemistry 41, 1171–1175.

Peterse, F., van der Meer, J., Schouten, S., Weijers, J.W.H., Fierer, N., Jackson, R.B., Kim, J.-H., Sinninghe Damsté, J.S., 2012. Revised calibration of the MBT–CBT paleotemperature proxy based on branched tetraether membrane lipids in surface soils. Geochimica et Cosmochimica Acta. doi:http://dx.doi.org/10.1016/j.gca.2012.08.011.

Powers, L.A., Werne, J.P., Johnson, T.C., Hopmans, E.C., Sinninghe Damsté, J.S., Schouten, S., 2004. Crenarchaeotal lipids in lake sediments: a new paleotemperature proxy for continental paleoclimate reconstruction? Geology 32, 613–616.

Powers, L.A., Johnson, T.C., Werne, J.P., Castañeda, I.S., Hopmans, E.C., Sinninghe Damsté, J.S., Schouten, S., 2005. Large temperature variability in the southern African tropics since the last glacial maximum. Geophysical Research Letters 32, L08706-1–L08706-4.

Powers, L.A., Werne, J.P., Vanderwoude, A.J., Sinninghe Damsté, J.S., Hopmans, E.C., Schouten, S., 2010. Applicability and calibration of the TEX_{86} paleothermometer in lakes. Organic Geochemistry 41, 404–413.

Rueda, G., Rosell-Melé, A., Escala, M., Gyllencrentz, R., Backman, J., 2009. Comparison of instrumental and GDGT-based estimates of sea surface and air temperatures from the Skagerrak. Organic Geochemistry 40, 287–291.

Schouten, S., Hopmans, E.C., Pancost, R.D., Sinninghe Damsté, J.S., 2000. Widespread occurrence of structurally diverse tetraether membrane lipids: evidence for the ubiquitous presence of low-temperature relatives of hyperthermophiles. Proceedings of the National Academy of Sciences of the USA 97, 14421–14426.

Schouten, S., Hopmans, E.C., Schefuß, E., Sinninghe Damsté, J.S., 2002. Distributional variations in marine crenarchaeotal membrane lipids: a new tool for reconstructing ancient sea water temperatures? Earth and Planetary Science Letters 204, 265–274.

Schouten, S., Hopmans, E.C., Kuypers, M.M.M., Bteugel, Y., Forster, S., Sinninghe Damsté, J.S., 2003. Extreme high sea water temperature at low latitudes during the middle Cretaceous as revealed by archaeal membrane lipids. Geology 31, 1069–1072.

Schouten, S., van der Meer, M.T.J., Hopmans, E.C., Rijpsrtra, W.I.C., Reysenbach, A-L., Ward, D.M., Sinninghe Damsté, J.S., 2007. Archaeal and bacterial glycerol dialkyl glycerol tetraether lipids in hot springs of Yellowstone National Park. Applied and Environmental Microbiology 73, 6181–6191.

Schouten, S., Hopmans, E.C., Baas, M., Boumann, H., Standfest, S., Konneke, M., Stahl, D.A., Sinninghe Damsté, J.S., 2008. Intact membrane lipids of "Candidatus Nitrosopumilusmaritimus", a cultivated representative of the cosmopolitan mesophilic Group I Crenarchaeota. Applied Environmental Microbiology 74, 2433–2440.

Schouten, S., Hopmans, E.C., Sinninghe Damsté, J.S., 2013. The organic geochemistry of glycerol dialkyl glycerol tetraether lipids: a review. Organic Geochemistry 54, 19–61.

Shi, G.Y., Xu, Q.X., Chen, Z.F., 2002. Analysis on channel scouring and silting and selfadjusting in mainstream and downstream reaches of Changjiang River. Journal of Mountain Science 20, 257–265 (in Chinese).

Sinninghe Damsté, J.S., Hopmans, E.C., Pancost, R.D., Schouten, S., Geenevasen, J.A.J., 2000. Newly discovered non-isoprenoid glycerol dialkyl glycerol tetraether lipids in sediments. Chemical Communications, 1683–1684.

Sinninghe Damste, J.S., van Duin, A.C.T., Geenevasen, J.A.J., 2002. Crenarchaeol: the characteristic core glycerol dibiphatanyl glycerol tetraether membrane lipid of cosmopolitan pelagic crenarchaeota. Journal of Lipid Research 43, 1641–1651.

Sinninghe Damsté, J.S., Ossebaar, J., Abbas, B., Schouten, S., Verschuren, D., 2009. Fluxes and distribution of tetraether lipids in an equatorial African lake: constraints on the application of the TEX_{86} palaeothermometer and BIT index in lacustrine settings. Geochimica et Cosmochimica Acta 73, 4232–4249.

Sinninghe Damsté, J.S., Rijpstra, W.I.C., Hopmans, E.C., Weijers, J.W.H., Foesel, B.U., Overmann, J., Dedysh, S.N., 2011. 13,16-Dimethyl octacosanedioic acid (iso-diabolic acid): a common membrane-spanning lipid of Acidobacteria subdivisions 1 and 3. Applied and Environmental Microbiology 77, 4147–4154.

Sinninghe Damsté, J.S., Ossebaar, J., Schouten, S., Verschuren, D., 2012. Distribution of tetraether lipids in the 25-ka sedimentary record of Lake Challa: extracting reliable TEX_{86} and MBT/CBT palaeotemperatures from an equatorial African lake. Quaternary Science Reviews 50, 43–54.

Smith, R.W., Bianchi, T.S., Li, X.X., 2012. A re-evaluation of the use of branched GDGTs as terrestrial biomarkers: implications for the BIT index. Geochimica et Cosmochimica Acta 80, 14–29.

Sun, Q., Chu, G.Q., Liu, M.M., Xie, M.M., Li, S.Q., Ling, Y., Wang, X.H., Shi, L.M., Jia, G.D., Lü, H.Y., 2011. Distributions and temperature dependence of branched glycerol dialkyl glycerol tetraethers in recent lacustrine sediments from China and Nepal. Journal of Geophysical Research 116, G01008. http://dx.doi.org/10.1029/2010JG001365.

Tierney, J.E., Russell, J.M., 2009. Distributions of branched GDGTs in a tropical lake system: implications for lacustrine application of the MBT/CBT paleoproxy. Organic Geochemistry 40, 1032–1036.

Tierney, J.E., Russell, J.M., Eggermont, H., Hopmans, E.C., Verschuren, D., Sinninghe Damsté, J.S., 2010. Environmental controls on branched tetraether lipid distributions in tropical East African lake sediments. Geochimica et Cosmochimica Acta 74, 4902–4918.

Tierney, J.E., Schouten, S., Pitcher, A., Hopmans, E.C., Sinninghe Damsté, J.S., 2012. Core and intact polar glycerol dialkyl glycerol tetraethers (GDGTs) in Sand Pond, Warwick, Rhode Island (USA): insights into the origin of lacustrine GDGTs. Geochimica et Cosmochimica Acta 77, 561–581.

Walling, D.E., Fang, D., 2003. Recent trends in the suspended sediment loads of the world's rivers. Global and Planetary Change 39, 111–126.

Walsh, E.M., Ingalls, A.E., Keil, R.G., 2008. Sources and transport of terrestrial organic matter in Vancouver Island Fjords and the Vancouver–Washington Margin: a multiproxy approach using $\delta^{13}C_{org}$, lignin phenols, and the ether lipid BIT index. Limnology and Oceanography 53, 1054–1063.

Wang, F., Yang, Z., Wang, Y., Saito, Y., Liu, J.P., 2008. Reconstruction of sediment flux from the Changjiang (Yangtze River) to the sea since the 1860s. Journal of Hydrology 349, 318–332.

Wang, H.Y., Liu, W.G., Zhang, C.L., Wang, Z., Wang, J.X., Liu, Z.H., Dong, H.L., 2012. Distribution of glycerol dialkyl glycerol tetraethers in surface sediments of Lake Qinghai and surrounding soil. Organic Geochemistry 47, 78–87.

Weijers, J.W.H., Schouten, S., van der Linden, M., van Geel, B., Sinninghe Damsté, J.S., 2004. Water table related variations in the abundance of intact archaeal membrane lipids in a Swedish peat bog. FEMS Microbiology Letters 239, 51–56.

Weijers, J.W.H., Schouten, S., Hopmans, E.C., Geenevasen, J.A.J., David, O.R.P., Coleman, J.M., Pancost, R.D., Sinninghe Damsté, J.S., 2006a. Membrane lipids of mesophilic anaerobic bacteria thriving in peats have typical archaeal traits. Environmental Microbiology 8, 648–657.

Weijers, J.W.H., Schouten, S., Spaargaren, O.C., Sinninghe Damsté, J.S., 2006b. Occurrence and distribution of tetraether membrane in soils: implications for the use of the BIT index and the TEX_{86} SST proxy. Organic Geochemistry 37, 1680–1693.

Weijers, J.W.H., Schefuß, E., Schouten, S., Sinninghe Damsté, J.S., 2007a. Coupled thermal and hydrological evolution of tropical Africa over the last deglaciation. Science 315, 1701–1704.

Weijers, J.W.H., Schouten, S., vandenDonker, J.C., Hopmans, E.C., Sinninghe Damsté, J.S., 2007b. Environmental controls on bacterial tetraether membrane lipid distribution in soils. Geochimica et Cosmochimica Acta 71, 703–713.

Weijers, J.W.H., Schouten, S., Schefuβ, E., Schneider, R.R., Sinninghe Damsté, J.S., 2009. Disentangling marine, soil and plant organic carbon contributions to continental margin sediments: a multi-proxy approach in a 20,000 year sediment record from the Congo deep-sea fan. Geochimica et Cosmochimica Acta 73, 119–132.

Weijers, J.W.H., Bernhardt, B., Peterse, F., Werne, J.P., Dungait, J.A.J., Schouten, S., Sinninghe Damsté, J.S., 2011. Absence of seasonal patterns in MBT–CBT indices in mid-latitude soils. Geochimica et Cosmochimica Acta 75, 3179–3190.

Wuchter, C., Schouten, S., Coolen, M.J.L., Sinninghe Damsté, J.S., 2004. Temperature-dependent variation in the distribution of tetraether membrane lipids of marine Crenarchaeota: implications for TEX_{86} paleothermometry. Palaeoceanography 19, PA4028.

Wuchter, C., Schouten, S., Wakeham, S.G., Sinninghe Damsté, J.S., 2005. Temporal and spatial variation in tetraether membrane lipids of marine Crenarchaeota in particulate organic matter: implications for TEX86 paleothermometry. Palaeoceanography 20, PA3013.

Wuchter, C., Herfort, L., Coolen, M.J.L., Abbas, B., Timmers, P., Strous, M., Herndl, G.J., Middelburg, J.J., Schouten, S., Sinninghe Damsté, J.S., 2006. Archaeal nitrification in the ocean. Proceedings of the National Academy of Sciences of the USA 103, 12317–12322.

Xie, S.C., Pancost, R.D., Chen, L., Evershed, R.P., Yang, H., Zhang, K.X., Huang, J.H., Xu, Y.D., 2012. Microbial lipid records of highly alkaline deposits and enhanced aridity associated with significant uplift of the Tibetan Plateau in the Late Miocene. Geology 40, 291–294.

Xu, K.H., Milliman, J.D., 2009. Seasonal variations of sediment discharge from the Yangtze River before and after impoundment of the Three Gorges Dam. Geomorphology 104, 276–283.

Yang, G.F., Chen, Z.Y., Yu, F.L., Wang, Z.H., Zhao, Y.W., Wang, Z.Q., 2007. Sediment rating parameters and their implications: Yangtze River, China. Geomorphology 85, 166–175.

Yang, H., Ding, W.H., Wang, J.X., Jin, C.S., He, G.Q., Qin, Y.M., Xie, S.C., 2012. Soil pH impact on microbial tetraether lipids and terrestrial input index (BIT) in China. Science China, Earth Sciences 55, 236–245.

Yao, Q.Z., Zhang, J., Wu, Y., Xiong, H., 2007. Hydrochemical processes controlling arsenic and selenium in the Changjiang River (Yangtze River) system. Science of the Total Environment 377, 93–104.

Zhang, C.L., Pearson, A., Li, Y.L., Mills, G., Wiegel, J., 2006. Thermophilic temperature optimum for crenarchaeol synthesis and its implication for archaeal evolution. Applied and Environment Microbiology 72, 4419–4422.

Zhang, C.L., Wang, J., Wei, Y., Zhu, C., Huang, L., Dong, H., 2012. Production of branched tetraether lipids in the lower Pearl River and estuary: effects of extraction methods and impact on bGDGT proxies. Frontiers in Microbiology 2. http://dx.doi.org/10.3389/fmicb.2011.00274.

Zhu, C., Weijers, J.W.H., Wagner, T., Pan, J.M., Chen, J.F., Pancost, R.D., 2011. Sources and distributions of tetraether lipids in surface sediments across a large river-dominated continental margin. Organic Geochemistry 42, 376–386.

Zink, K.-G., Vandergoes, M.J., Mangelsdorf, K., Dieffenbacher-Krall, A.C., Schwark, L., 2010. Application of bacterial glycerol dialkyl glycerol tetraethers (GDGTs) to develop modern and past temperature estimates from New Zealand lakes. Organic Geochemistry 41, 1060–1066.